# Ellipsoidal deformation of vertical quantum dots

D. G. Austing,* S. Sasaki, and S. Tarucha†
*NTT Basic Research Laboratories, 3-1 Morinosato Wakamiya, Atsugi, Kanagawa 243-0198, Japan*

S. M. Reimann,‡ M. Koskinen, and M. Manninen
*Physics Department, University of Jyväskylä, P.O. Box 35, 40351 Jyväskylä, Finland*
(Received 17 May 1999)

Addition energy spectra at 0 T of circular and ellipsoidally deformed few-electron vertical quantum dots are measured and compared to results of model calculations within spin-density-functional theory. Because of the rotational symmetry of the lateral harmonic confining potential, circular dots show a pronounced shell structure. With the lifting of the single-particle level degeneracies, even a small deformation is found to radically alter the shell structure leading to significant modifications in the addition energy spectra. Breaking the circular symmetry with deformation also induces changes in the total spin. This ''piezomagnetic'' behavior of quantum dots is discussed, and the addition energies for a set of realistic deformation parameters are provided. For the case of the four-electron ground state at 0 T, a spin-triplet to spin-singlet transition is predicted, i.e., Hund's first rule no longer applies. Application of a magnetic field parallel to the current confirms that this is the case, and also suggests that the anisotropy of an elliptical dot, in practice, may be higher than that suggested by the geometry of the device mesa in which the dot is located. [S0163-1829(99)05839-7]

## I. INTRODUCTION

In atomic physics, the mean-field method describing the motion of electrons confined in the three-dimensional spherically symmetric Coulomb potential of the nucleus provides an impressively powerful tool to explain the chemical inertness and special stability of the noble gases. The well-known atomic shell structure is a consequence of the fact that the atomic levels $1s,2s,2p,3s,3p, \ldots$ show a ''bunchiness'' in their distribution as a function of energy. Particular stability of the electronic system is reached when a bunch of such levels is fully occupied. If then one more electron is added, the electron configuration would involve a singly occupied orbital from the next higher shell, and consequently, the system is then less stable. Shell filling is thus reflected by large maxima in the ionization energy for atomic numbers 2,10,18, . . . , corresponding to the nobel gas atoms He, Ne, Ar, . . . . In the mid-shell regions, large level degeneracies occur as a consequence of the spherical symmetry of the confining potential of the atomic nucleus. The midshell levels are then filled according to Hund's rules, in particular maximizing the total electron spin for half-filled orbitals.[1]

A shell structure is not only unique to atoms, but actually is a recurring property in finite fermion systems with high symmetry.[2] It equally explains the occurrence of ''magic'' proton and neutron numbers in the binding energies of nuclei, and more recently the discovery of ''magic'' atom numbers in metal clusters[3]—small aggregates of metal atoms in which delocalized valence electrons move in the positive charge background of the ions. Fundamentally, in contrast to atoms, however, both midshell nuclei and clusters deform their mean field rather than obey Hund's rules.

The two-dimensional analogue to the atom with its static $1/r$ radial Coulomb confinement due to the nucleus can be realized in small semiconductor devices: artificial semiconductor atoms based on quantum dot technology. Clean, well-defined, and highly symmetric vertical quantum dots (''islands'') can now be made so small that the dot size is comparable to the Fermi wavelength.[4–6] Typical micrographs of micron-sized device mesas incorporating these dots are shown in Fig. 1. The lateral electrostatic confinement originates from side-wall depletion, and this (and the effective dot size) can be controlled or ''squeezed'' by the action of a Schottky gate wrapped around the mesa in the vicinity of the dot to the degree that the number of electrons trapped on the dot can be changed one by one. Also the

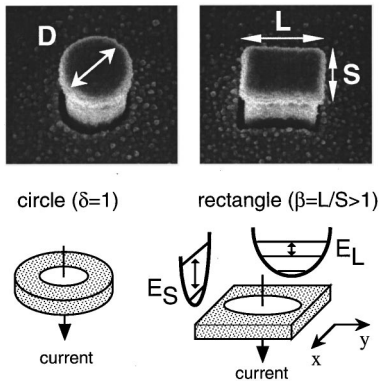


FIG. 1. Typical scanning electron micrographs show a circular mesa with top contact diameter $D$, and a rectangular mesa with top contact area $L \times S$ $(L > S)$ taken immediately after the deposition of the Schottky gate metal surrounding the mesa. The slight undercut due to the light wet etch is clearly visible. Schematic diagrams depict the slabs of semiconductor between the two tunneling barriers, and the resulting circular and elliptical shaped dots bounded by the shaded depletion region for the circular and rectangular mesas, respectively. The current flows vertically through the dots in the direction indicated. For the rectangular mesa, the energy parabola along the major and minor axes are included and the respective confinement energies, $E_L$ and $E_S(E_L < E_S)$, are marked.

 

few-electron regime is readily accessible, and then the resulting confinement is well approximated by a parabolic $r^2$ potential. Electron phenomena in related semiconductor quantum dot structures continue to attract much attention.[7–9] As they exhibit atomiclike properties, such as a shell structure and shell filling in accordance with Hund's first rule, the vertical quantum dots, whose heterostructure barriers are both abrupt and thin, can be regarded as artificial atoms whose ground and excited states can be probed electrically by single-electron tunneling spectroscopy in order to perform novel ''atomic physics'' experiments in the few-electron regime.[10,11]

When an arbitrarily small bias $V$ is applied across the dot between the metal contact on top of the device mesa and the substrate contact (these are often refered to as the source and drain contacts), the ground states of an $N$-electron quantum dot weakly coupled to the contacts can be investigated directly by monitoring the current flowing vertically through the dot at or below 0.3 K as the voltage $V_g$ on a single gate surrounding the dot is varied. When no current flows (Coulomb blockade), $N$ is well defined. On the other hand, when current flows the number of electrons can oscillate between $N$ and $N+1$. With the gate, $N$ can be increased one by one starting from zero by making $V_g$ more positive, so a series of sharp current peaks due to the charging of the dot (Coulomb oscillations) can be observed. For a large dot containing many electrons, the Coulomb oscillations are usually periodic because the single-electron charging energy is determined classically just by the total dot capacitance. For a dot containing just a few electrons both quantum effects reflecting the underlying symmetry of the confining potential, and the details of the electron-electron interactions become important as the dot size is reduced. This leads to modifications of the Coulomb oscillations, so they are no longer expected to be periodic.[6,10]

To date, we have mainly focused on the properties of dots in circular mesas that have diameters of typically 0.4 to 0.7 microns. For a magnetic field parallel to the current, the measured ground states between 0 T and about 4 T for $N<20$ in these disk-shaped dots can be well accounted for by a single-particle picture based on the Darwin-Fock spectrum for a circular two-dimensional harmonic confining potential, a constant interaction, and corrections at 0 T due to exchange, i.e., Hund's first rule.[6,10] At higher fields beyond about 4 T, the evolution of ground states (and also the excited states) for $N<6$ can be understood in terms of many-body effects.[11]

The main theme of this paper concerns the effect of geometrically distorting a circular dot into an elliptical (anisotropic) dot. Previously, we have briefly reported some properties of elliptical dots.[6,12] Here, we present a more detailed study of the addition energies and include their magnetic-field dependencies. The experimental data are compared to model calculations. We survey general trends, and examine basic assumptions about the nature of the deformed dots.

A perfectly circular dot possesses full rotational symmetry. This high symmetry leads to maximal level degeneracy of the single-particle two-dimensional states for parabolic confinement, and this emphasises atomiclike properties.[6] This level degeneracy at 0 T for a circular dot is evident in the single-particle spectrum in Fig. 2(a), and consecutive filling of each set of degenerate states is directly responsible for

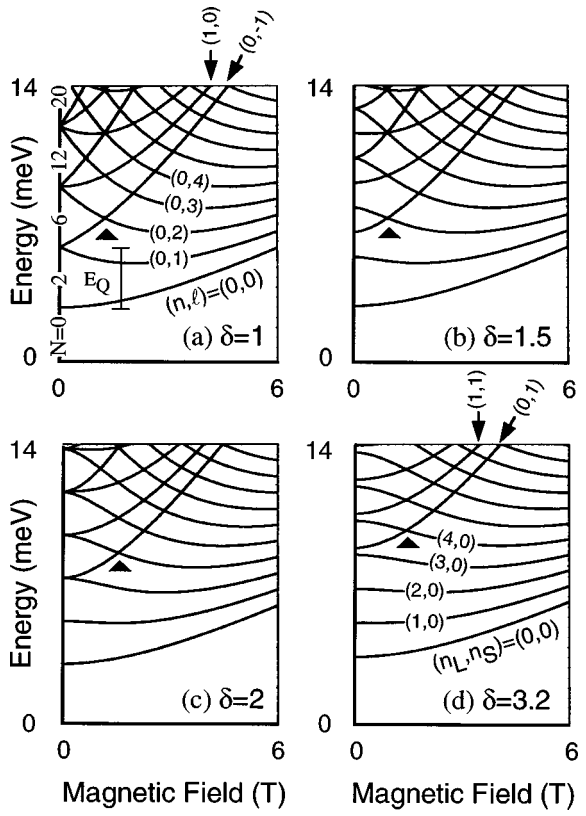


FIG. 2. Magnetic ($B$-) field dependence up to 6 T of the first ten single-particle energy levels (each level can hold a spin-up and spin-down electron) for a circular dot with $\delta=1$, (a), and for elliptical dots with $\delta=1.5$, 2, and 3.2, (b) to (d). The energy level spectra are calculated with the simple formalism employed by Madhav and Chakraborty, as explained in the text. The spectrum for the circular dot is in fact the familiar Darwin-Fock spectrum for a circular two-dimensional perfectly harmonic confining potential. The confinement energy for the circular dot $E_Q$, is taken to be 3 meV, a reasonable average value in the few-electron limit, and is assumed to be independent of $N$. The confinement energies for the elliptical dots are simply derived from the relation $E_L E_S = E_Q E_Q$. For the circular dot and the $\delta=3.2$ ellipse, quantum numbers $(n,l)$ and $(n_L,n_S)$ respectively, for some states are given. At 0 T accidental degeneracies are also evident for the $\delta=1.5$ and $\delta=2$ ellipses, but not for the $\delta=3.2$ ellipse. The black triangles mark the position of the first (lowest energy) single-particle crossings.

the characteristic shell structure with ''magic'' numbers $N=2,6,12,20,\ldots$. Furthermore, Hund's first rule accounts for the parallel filling of electrons amongst half-filled degenerate states in a shell at numbers $N=4,9,16,\ldots$ due to an exchange effect. Breaking the circular symmetry by deforming the lateral confining potential lifts the degeneracies of the single-particle levels present in a disk-shaped dot. This destroys the shell structure for a circle, and modifies other atomiclike properties.[13]

The sequence of spectra in Fig. 2 also introduces two key points in our subsequent arguments. Firstly, as the deformation is gradually increased, Figs. 2(a) to 2(d), degeneracies of the single-particle states at 0 T are generally removed. Nevertheless, accidental degeneracies can occur at certain ''magic'' deformations, e.g., Figs. 2(b) and 2(c), leading to subshell closures, provided the confining potential is still perfectly parabolic. The resulting patterns, however, are very

different from that for the circular case, Fig. 2(a), and in practice may be hard to observe. Secondly, a weak-magnetic field parallel to the current can also induce level degeneracies in both circular and elliptical dots when single-particle levels cross at finite field, but here too, any shell structure at a particular field is of a lower order and less apparent than that for the circle at 0 T.[13]

While illustrative, ultimately any modeling of the behavior of real dots must go beyond a system of $N$ noninteracting electrons confined by a two-dimensional harmonic oscillator, i.e., a single-particle picture, as employed to generate the spectra in Fig. 2,[13] and include Coulomb interactions which can lift certain degeneracies at 0 T. Numerical diagonalization of the full Hamiltonian matrix has recently been successfully employed to calculate basic electronic properties of dots with anisotropic confining potentials.[14,15] Such ''exact'' numerical calculations, however, are limited to only a few confined particles. In order to study dots confining a larger number of electrons we apply spin-density-functional theory at 0 T. This powerful technique, which explicitly incorporates the electron-spin interactions, has lead to a number of interesting predictions for the ground-state structure of quantum dots, although there is a continuing discussion as to the interpretation of so-called spin-density waves (SDW).[16–21] Both ''exact'' numerical calculations and spin-density-functional theory predict subtle changes in the addition energy spectra, and transitions in the spin states as deformation is varied—even for a weak deformation. An example of the latter is the breakdown of the conditions for which Hund's first rule applies for four electrons, and this marks a transition from a spin-triplet to a spin-singlet configuration, i.e., states are consecutively filled by spin-up and spin-down electrons.

## II. EXPERIMENT SETUP

The vertical quantum dots under focus in the following are fabricated by electron-beam lithography, and a two step etching technique to make circular or rectangular submicron mesas from one special GaAs/$Al_{0.22}Ga_{0.78}As$/$In_{0.05}Ga_{0.95}As$/$Al_{0.22}Ga_{0.78}As$/GaAs double barrier heterostructure (DBH). Full details of the device fabrication, and the material parameters are given elsewhere.[4–6,10] A single Schottky gate is placed around the side of the mesa close to the DBH. We discuss one circular mesa with a nominal top contact diameter $D$, of 0.5 $\mu$m (W), and three rectangular mesas with a top contact area $(L\times S)$ $0.55\times0.4\,\mu m^2$ $(X)$, $0.65\times0.45\,\mu m^2$ $(Y)$, and $0.6\times0.4\,\mu m^2$ $(Z)$. $L(S)$ is the nominal dimension of longest (shortest) side of the top contact. Figure 1 shows typical scanning electron micrographs of a circular mesa, and a rectangular mesa taken immediately after the depositon of the Schottky gate metal surrounding the mesa. For the rectangular mesas, an intuitively simple way to classify them is to define a geometric parameter $\beta$, to be the ratio $L/S$. For $X$, $Y$, and $Z$, respectively $\beta$ is nominally 1.375, 1.44, and 1.5. Due to a slight isotropic undercut resulting from the light wet etch during the formation of the mesa,[4,5] the area of the mesas, as revealed by the micrographs, is a little less than that of the top contact, so realistic values for $\beta$ are estimated to be about 5% larger than the values quoted.

Figure 1 also schematically shows the slabs of semiconductor between the two $Al_{0.22}Ga_{0.78}As$ tunneling barriers, and the resulting dots bounded by the shaded depletion region for the circular and rectangular mesas. The thickness of the $In_{0.05}Ga_{0.95}As$ slab is determined by the separation between the well-defined heterostructure tunneling barriers (approximately 100 Å). The slab is sufficiently thin that all electrons are in the lowest state in the vertical direction parallel to the current. The lateral confining potential due to the side wall depletion further restricts electrons to the center of the slab, thus defining the dot region. We note that in our devices, the extent of the lateral depletion region in the vicinity of the dot is largely determined by the electron density in the $n$-doped GaAs regions above and below.

The lateral harmonic confining potential of the dot in the circular mesa has circular symmetry of a sufficiently high degree that degenerate sets of states can systematically form in the disk-shaped dot.[6] These states can be labeled by the quantum numbers $(n,l)$, where $n$ is the radial quantum number $(=0,1,2,\ldots)$, and $l$ is the angular momentum quantum number $(=0,\pm1,\pm2,\ldots)$. Each state can hold a spin-up electron and a spin-down electron. At 0 T the $2n+|l|+1$th shell is made up of $2n+|l|+1$ degenerate single-particle states. Each degenerate set of states can be regarded as a shell of an artificial atom, and this is the origin of the 2,6,12,20, ... ''magic'' numbers. The first shell consists of the (0,0) level, the second shell of the (0,1) and $(0,-1)$ levels, the third shell of the (0,2), (1,0), and $(0,-2)$ levels, and so on. For the circular dots we typically study, the lateral electrostatic confinement energy seperating these degenerate sets of single-particle states $E_Q$ can be as large as 5 meV in the few-electron limit.[11] Neglecting an arbitrary constant, the energy of single-particle state $(n,l)$ is $(2n+|l|+1)E_Q$. The effective lateral diameter can be ''squeezed'' from a few thousand Angstroms for $N$ of approximately 100 down to 0 Å for $N=0$ by making the gate voltage more negative.[6,10,11] We stress that crucially the ''squeezing'' action of the gate, and indeed application of a magnetic field parallel to the current, preserves the circular symmetry of a disk-shaped dot. Consequently, atomiclike properties should be particularly robust and evident in circular dots.

For a rectangular mesa, the lateral confining potential of the dot is expected to be elliptical-like due to rounding at the corners provided the number of electrons in the dot is not too large (in which case it may be more rectangularlike with rounded corners), or too small. Right at ''pinch-off'', $(N\rightarrow0)$, it may even become more circularlike, i.e., the elliptical shape of the confining potential may be changing in a complex way.[6,12] Assuming the confining potential is perfectly parabolic, we can choose to characterize the ''ellipticity'' by a deformation parameter, $\delta=E_S/E_L$. Here, $E_S(E_L)$ is the confinement energy at 0 $T$ along the minor (major) axis $(E_S>E_L)$. The states in the elliptical dot are now labeled by the quantum numbers $(n_L,n_S)$, where $n_L$ $(n_S)$ is a quantum number $(=0,1,2,\ldots)$ associated with the energy parabola along the major (minor) axis.[13] Again neglecting an arbitrary constant, the energy of single-particle state $(n_L,n_S)$ is $(n_L+1/2)E_L+(n_S+1/2)E_S$.

For a perfectly circular mesa, we can trivially generalize our definition of the deformation parameter so that $\delta=\beta=1$. On the other hand, for the rectangular mesas, there is no simple correspondance between $\beta$, a ratio of lengths charac-

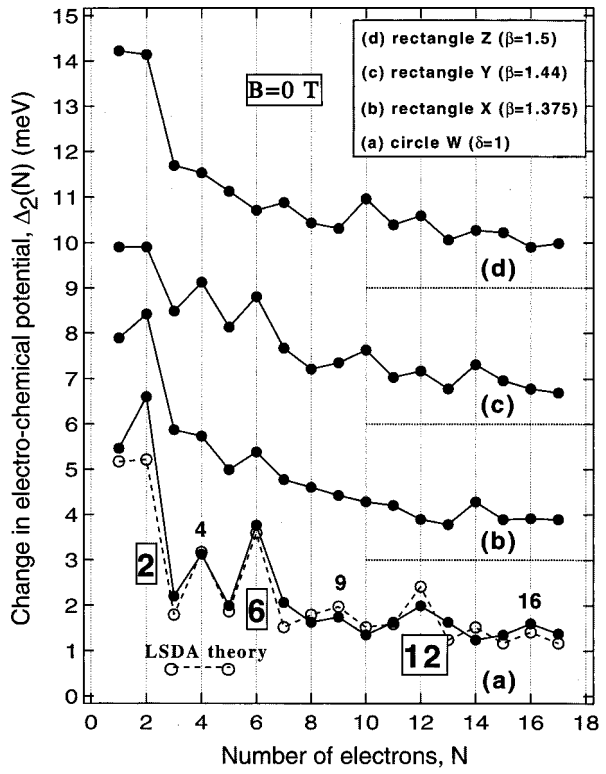


FIG. 3. Change in the electrochemical potential, $\Delta_2(N)$, as a function of electron number $N$, up to 17 at 0 T for circular mesa $W$ of diameter 0.5 $\mu$, (a), and three rectangular mesas $X$, $Y$, and $Z$ of area $0.55\times0.4$, $0.65\times0.45$, and $0.6\times0.4\,\mu\mathrm{m}^2$, respectively, (b) to (d). For $W$, $\delta=1$, and for $X$, $Y$, and $Z$, respectively, $\beta$ is nominally 1.375, 1.44, and 1.5. The traces are offset vertically by 3 meV for clarity. For circular dot $W$, a clear shell structure is observed. Peaks due to full ($N=2,6,12$) and half-full ($N=4,9,16$) shell filling are numbered, and the fit given by local spin-density approximation (LSDA) is included, as discussed in the text and also shown in Fig. 4.

teristic of the top metal contact which is independent of gate voltage (or $N$), and $\delta$, a ratio of energies characteristic of the dot in the mesa, which is in fact dependent on the gate voltage (or equivalently $N$), i.e., ''accidental'' degeneracies at ''magic'' deformations will be hard to see over an extended range of $N$, and in any case may be lifted if the confinement potential is not completely parabolic. Nevertheless, at this stage, we start by assuming that $\beta$ is a measure of $\delta$, and thus one might expect $\delta_Z>\delta_Y>\delta_X>\delta_W$. We are not saying that $\delta=\beta$ for the ellipses, and indeed even for the simplest possible model of uniform depletion spreading due to the action of the gate, we would expect $\beta$ to underestimate $\delta$. We furthermore assume in the following model calculations, for simplicity, that the ''squeezing'' action of the gate does not alter $\delta$. We will examine these assumptions in light of the experimental and theoretical data presented. Note that the application of a magnetic field parallel to the current effectively reduces $\delta$ as seen by the confined electrons in the limit of a very high field, where it approaches unity.

### III. ADDITION ENERGY SPECTRA FOR CIRCULAR AND DEFORMED DOTS

In Fig. 3, the change (formally the second difference) in the electrochemical potential, $\mu(N+1)-\mu(N)=\Delta_2(N)$, which can also be regarded as a capacitive energy,[16] is plotted as a function of electron number $N$, up to $N=17$ for (a) $W$, (b) $X$, (c) $Y$, and (d) $Z$ at 0 T. The traces are offset vertically by 3 meV for clarity. The $N$th current peak position in gate voltage $V_g$, at a very small bias ($\ll$1 mV), i.e., measured in the linear conductance regime, at or below 0.3 K reflects $\mu(N)$, the electrochemical potential of the ground state for $N$ electrons, or equivalently the ''addition energy'' to place an extra electron on a dot with $N-1$ electrons. $\Delta_2(N)$ then mirrors directly the spacing in gate voltage between the $N+1$th and the $N$th current peaks.[10] $\Delta_2(N)$ is actually the half width of the $N$th Coulomb diamond, the diamond-shaped region in the $V$-$V_g$ plane in which current is blocked between the $N$th and the $N+1$th current peaks. $\Delta_2$ contains contributions from the single-electron charging energy and changes in the single-particle energy $E_Q$.[10,11]

At 0 T, for the circle $W$, $\Delta_2(N)$ is strongly dependent on $N$, and a very clear characteristic shell structure is evident in Fig. 3(a).[10] Particularly large peaks ($N=2,6,12$) and relatively large peaks ($N=4,9,16$) are indicated. The result from a local spin density approximation calculation discussed below is also included for comparison.[20] $N=2$, 6, and 12 are the first three ''magic'' numbers for a circular two-dimensional harmonic potential which mark completion of the first three shells (containing respectively 1, 2, and 3 degenerate zero-dimensional single-particle states or equivalently 2, 4, and 6 electrons). The peaks at $N=4,9,16$ arise as a consequence of exchange effects, which are enhanced at half-shell filling with same-spin electrons for the second, third, and fourth shells respectively.[10] This shell structure should be clear (and this is generally the case in practice for $N<20$) as long as: (i) the two-dimensional lateral potential remains radially parabolic, and rotationally symmetric to a fairly high degree, (ii) $E_Q$ is comparable to, or larger than, the Coulomb interaction energy, and (iii) the effect of screening is not significant.

For the circular mesa $W$, it is also evident that as $N$ is decreased, $\Delta_2(N)$ generally becomes larger due to the increase of the Coulomb interaction when the dot is ''squeezed.'' This observation also holds for the rectangular mesas, but there are no prominant maxima at $\Delta_2(2,6,12)$. The shell structure for the disk-shaped dot has now become disrupted or ''smeared out,'' and this can be attributed directly to the lifting of the degeneracies of the single-particle states that are present in a circular dot.[6,10,12] In other words, deformation kills the shell structure for a circle, and even quite a small deformation can make a big difference. This is evident from the three traces, (b) to (d) in Fig. 3, but there are major difficulties in discussing specific details. As noted earlier, in practice, right at ''pinch-off'', $\delta$ may actually tend towards unity,[6,12] but more generally $\delta\approx\beta$ may be unreliable. Also, even for two circular dots, which have a clear shell structure in the few-electron limit, the absolute values of $\Delta_2(N)$ can vary from dot to dot, i.e., the precise details are device dependent, and beyond the third shell only a few devices show the expected behavior clearly.[10] Lastly, even if $\delta$ could be determined accurately, $\Delta_2(N)$ strictly speaking can only be fairly compared if the ''areas'' of the dots are comparable, as in the classical limit $\Delta_2(N)$ is determined by the overall dot capacitance.[6] Based on the nominal sizes of

the mesas, and in line with the trends of the ''pinch-off'' gate voltage as identified by the position of the first current peak, elliptical dots *X*, *Y*, and *Z*, respectively may have ''areas'' 1.1, 1.5, and 1.2 larger than that of the circular dot *W*. Thus to sensibly discuss details, like the spin-states, even generally, we first calculate $\Delta_2(N)$ at 0 T for a range of $\delta$ values in line with those suggested by the $\beta$ values of the mesas *X*, *Y*, and *Z*. We then compare with, and look for patterns in, the experimental data at 0 T, before looking at the magnetic-field dependence for confirmation of trends, and whether $\delta \approx \beta$ is reasonable.

## IV. MEAN-FIELD MODEL FOR CIRCULAR AND ELLIPTICAL QUANTUM DOTS

We next aim to model the changes due to the deformation of the lateral confinement to the shell structure of the quantum dots at 0 T by applying the methods of spin-density functional theory (SDFT). We will briefly address different aspects of the spin structure relevant to the deformed quantum dots.

### A. The method

To obtain the ground-state energies and densities for *N* electrons confined in an externally imposed potential, we solve the spin-dependent single-particle Kohn-Sham (KS) equations[22]

$$\left[ -\frac{\hbar^2}{2m^*}\nabla_{\mathbf{r}}^2 + V_{\mathrm{eff}}^{\sigma}(\mathbf{r}) \right] \psi_{i,\sigma}(\mathbf{r}) = \epsilon_{i,\sigma}\psi_{i,\sigma}(\mathbf{r}), \qquad (1)$$

in a plane-wave basis to avoid any symmetry restrictions. In Eq. (1), the index $\sigma$ accounts for the spin ($\uparrow$ or $\downarrow$), and $\mathbf{r} = (x,y)$. The effective mean-field potential, $V_{\mathrm{eff}}^{\sigma}(\mathbf{r})$, contains contributions from the external harmonic confining potential, the Hartree potential of the electrons, and the functional derivative of the local exchange-correlation energy, for which we use the approximation of Tanatar and Ceperley[23] (see also Refs. 17 and 20 for details). The electrostatic confinement due to the lateral depletion region imposed by the side wall and the Schottky gate is approximated by a two-dimensional anisotropic harmonic oscillator with frequencies $\omega_x = \omega\sqrt{\delta}$ and $\omega_y = \omega/\sqrt{\delta}$,

$$V_{\mathrm{ext}}(x,y) = \frac{1}{2}m^*\omega^2\left( \delta x^2 + \frac{1}{\delta}y^2 \right). \qquad (2)$$

The ratio of the oscillator frequencies, $\delta = \omega_x/\omega_y$, thus defines the ratio of semiaxes of the ellipsoidal equipotentials. We impose the constraint, $\omega^2 = \omega_x\omega_y$, which is equivalent to conserving the area of the quantum dot with deformation.[20] The *x* and *y* axes are indicated in the schematic diagram for the elliptical dot in Fig. 1. With this convention, the above-defined $E_S$ and $E_L$, respectively correspond to $\hbar\omega_x$ and $\hbar\omega_y$. In the model we present the dot is assumed to be well isolated from its surroundings, so any effects due to the presence of the gate and the neighboring conducting regions are neglected. Likewise, screening and nonparabolicity effects inside the dot, which become more important for large *N*, are not considered.

For $\delta = 1$, a circular shape for the quantum dot is obtained, whereas $\delta > 1$ corresponds to an ellipsoidally deformed quantum dot. The strength $\omega$ of the external parabolic confinement leading to an average particle density, $n_0 = 1/(\pi r_s^2)$, in a circular dot is approximated by $\omega^2 = e^2/(4\pi\epsilon_0\epsilon m^* r_s^3\sqrt{N})$.[17] Minimizing the energy density functional by self-consistently solving the above KS equations, Eq. (1), ground-state energies, $E(N,\delta)$, are obtained for different electron numbers and deformation parameters. Full technical details are given elsewhere,[17,20] and here we report only the results. We emphasise that from recent measurements, it is clear that as *N* increases the confinement weakens in such a way that the particle density tends to a constant.[24] This is implicit in our model, as for any given value of $r_s$, the oscillator frequency $\omega$, and the related frequencies $\omega_x$ and $\omega_y$, decrease with increasing *N*. $\delta$ is also kept constant for simplicity, although $\delta$ is expected to vary with *N* in practice.

Although strictly speaking the dot is located in $In_{0.05}Ga_{0.95}As$, we take for values of the effective mass $m^*$ and dielectric constant, $\epsilon$, those for GaAs—namely 0.067 and 13.1, respectively. There are no fitting parameters in the equations, and only a suitable choice for $r_s$ is required to generate the addition energy spectra. The value of $r_s = 1.5a_B^*$ used in the model calculations is realistic as the value estimated experimentally for a circular quantum dot is 1.3 to $1.4a_B^*$.[24] $a_B^* = \hbar^2(4\pi\epsilon_0\epsilon)/m^*e^2$ is an effective atomic unit, which for GaAs is about 103 Å. $r_s = 1.5a_B^*$ in the model presented here corresponds to an effective confinement energy, $E_Q$, for $N = 1$ of about 5.7 meV. This value is consistent with the upper limit of $E_Q$ observed in practice (about 5 meV), and justifies the $E_Q = 3$ meV value as a reasonable average for calculating the simple single-particle spectra shown in Fig. 2 for the first ten levels.

We point out that the SDFT calculations described here, as well as those performed by Hirose and Wingreen,[21] are strictly two dimensional, so the strength of the Coulomb interactions may be overestimated, i.e., the possibility of charge spreading out in both the *x*-*y* plane, and along the vertical direction parallel to the current to minimize the Coulomb energy is neglected. Equivalently, anisotropic extension of the electron wave functions along the major axis is ignored.[6] In practice, screening by the metal contacts surrounding a dot is also believed to reduce the influence of Coulomb interactions. The three-dimensional model of Lee *et al.*[16] does incorporate self-consistent solution of the Poisson equation into a SDFT calculation, but because they use different expressions for the exchange-correlation energy, and considerably higher values for $E_Q$, $E_L$, and $E_S$ (up to 20 meV), a direct comparison with their results is not easy. Nevertheless, they find that electrons strongly confined in the vertical direction have a very strong two-dimensional character, and both approaches lead to the same qualitative conclusions. Namely, the distinct shell structure for a circle, as well as the spin states, at 0 T are strongly modified with deformation.

### B. $\Delta_2(N)$ for elliptical dots: Results from LSDA calculations

We now make a simple comparison between the experimentally measured traces for the change in the electrochemi-

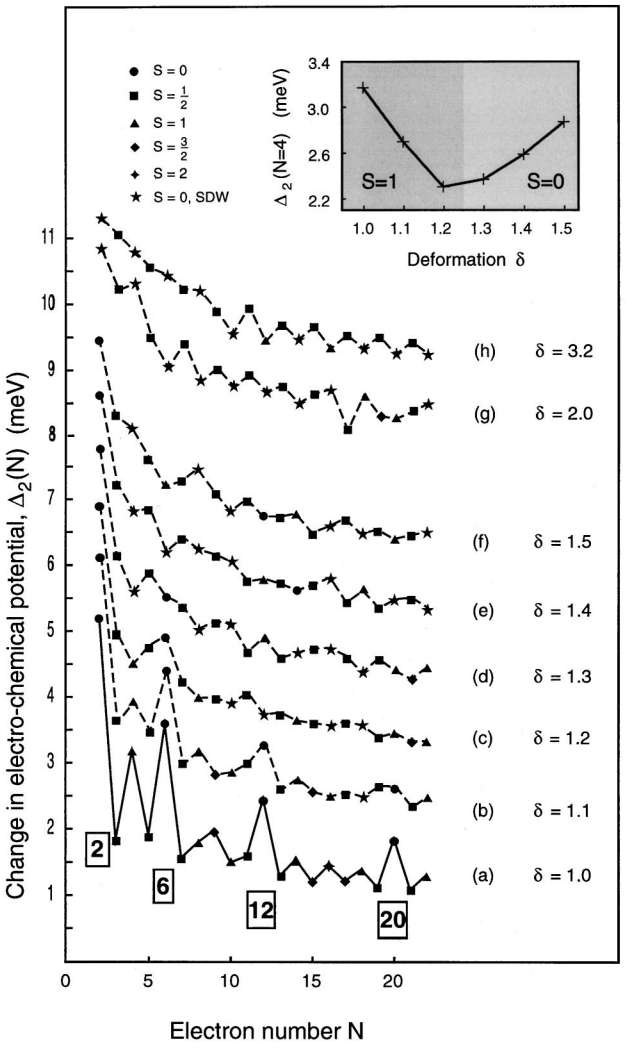


FIG. 4. Model calculations for the change in electrochemical potential, $\Delta_2(N)$, within spin-density-functional theory. The different traces correspond to zero, weak, and moderate deformation parameters $\delta=1.0$ to $\delta=1.5$, (a) to (f), and higher deformation parameters $\delta=2$ and $\delta=3.2$, (g) and (h). The traces are offset vertically by 1 meV for clarity, and there is an additional 1 meV offset between traces (f) and (g). Traces (a) to (f) illustrate well the dramatic destruction with deformation of the familiar shell structure for a circular dot. The total spin $S$ for different deformations and electron numbers are identified by different symbols as defined in the figure. Note that with increasing deformation, $S=0$ spin-density wave (SDW) states are predicted to become more prevalent for even $N$. The inset shows $\Delta_2(N=4)$ versus $\delta$. For $\delta<1.2$ and $\delta>1.3$, respectively, the $N=4$ ground state is expected to be a spin triplet ($S=1$) and spin singlet ($S=0$).

cal potential, $\Delta_2(N)$, with those modelled theoretically. Figure 4 shows $\Delta_2(N)$, derived from the self-consistent ground-state energies, $E(N,\delta)$. The energies are obtained by self-consistently solving the KS equations starting from different initial guesses for the effective KS potential for the spin-up and spin-down particles. The initial potentials are chosen completely arbitrarily by just putting small random numbers on to the lattice points. The calculations are started from four such guesses. For two of them, the spin-up and spin-down initial guesses are shifted in value in order to search for states with nonzero total spin for even $N$. This is important in order to find the ground state amongst all possible spin configurations with a high degree of certainty.[17,20]

The lowest trace in Fig. 4 gives $\Delta_2(N)$ for the circular dot ($\delta=1$, i.e., zero deformation). As expected, the circular-shaped confinement produces a spectrum with the familiar shell structure for a two-dimensional harmonic oscillator, with shell closures at the ''magic'' numbers 2, 6, 12, and 20. At the average particle density corresponding to $r_s=1.5a_B^*$, these ''magic'' numbers arise from large gaps at the Fermi surface and paired spins in each nondegenerate level, so the total spin is zero ($S=0$). We note that within this mean-field model, spin-density wave (SDW) states are not expected for these particular spin-zero states.[17,20]

In Fig. 3(a), for $\delta=1$, the experimental and theoretical traces can be directly compared. The agreement is strikingly good, given that no parameters are fitted to reproduce the experimental data. Not only are the principal peaks 2, 6, and 12 well reproduced, but the relatively large peaks at 4, 9, and 16 for the high-spin states at half-shell filling are also clear.[17,20] For $N=4$, Hund's first rule correctly predicts the calculated $S=1$ spin-triplet state in which spins are aligned in the two highest partially occupied degenerate single-particle levels $(n,l)=(0,1)$ and $(0,-1)$, rather than the $S=0$ spin-singlet state in which the paired-spin electrons reside in either the $(0,1)$ or $(0,-1)$ levels.

Deforming the confinement slightly by changing the deformation parameter to $\delta=1.1$ [see trace (b) in Fig. 4], the calculation still predicts fairly clear shell closures at $N=2$, 6, and 12. These numbers can still be considered as ''magic,'' but the actual values of $\Delta_2(2,6,12)$ are noticeably suppressed, because degeneracies have been lifted.[6] The $N=20$ peak has become very weak. Also values of $\Delta_2(N)$ neighboring $N=2$, 6, and 12 start to become comparable to the values for $N=2$, 6, and 12, i.e., there is less contrast. Overall, the shell structure is much less pronounced compared to that for the circle. Already it is clear that even a very small deviation from perfect circular symmetry can have a very noticeable effect even when single-particle level degeneracies are lifted by just a small amount.

As the deformation increases further, the pronounced peaks for $N=2$, 6, 12, and 20 evident for the disk-shaped dot are further suppressed. This is a simple consequence of the removal of the level ''bunching'' with deformation. Even for the cases where ''accidental'' subshell closures occur at certain ''magic'' deformations (e.g., $\delta=1.5$ and 2 as seen in Fig. 2), the reduced separation between degenerate single-particle energy levels ($E_L$) would make any shell structure less clear to observe, and the sequence of ''magic'' numbers would be very different (e.g., for $\delta=2$ it would be 2,4,8,12,18, . . . ) compared to those for $\delta=1$. From Fig. 4 we can see essentially that for $\delta\geqslant 1.2$, the circular shell structure has been completely eliminated. Traces (a) to (f) thus illustrate the dramatic destruction of the familiar shell structure for a circular dot with deformation.

Also apparent is that a systematic one-to-one correspondance of $\Delta_2(N)$ between traces (b) to (d) in Fig. 3 and traces (b) to (f) in Fig. 4 is impossible to make. Although the experimental data for mesa $X$ partly resembles the theoretical data for $\delta=1.1$ to 1.3, the data for mesas $Y$ and $Z$ do not seem to resemble that for $\delta>1.3$, except perhaps for a weak tendency to oscillate between even $N$ and odd $N$. We have

already stated many reasons why, in comparison to a circular dot, a good correspondance between experiment and theory for the elliptical dots is less likely. We stress that ultimately, except for circle *W*, $\delta$ is not known, and equating $\delta$ with $\beta$ may not be reliable. To progress we must look for other clues.

Theoretically, Fig. 4 shows that there are transitions in the ground-state spin configurations with deformation.[20] The total spin $S$ is identified by different symbols in the figure. These transitions are particularly numerous for, but are not restricted to, the even-$N$ systems, and are clearly very sensitive to the actual value of the deformation. For example, in the case of $N=6$ electrons, the total spin is predicted to change from $S=0$ (i.e., a paramagnetic state) at $\delta=1$, through an $S=0$ SDW state, to $S=1$ at $\delta=1.5$—an indication of ''piezo-magnetic'' behavior,[20,25] i.e., changes of the dot magnetization with deformation. Although experimentally we are not in a position to differentiate between an $S=0$ ''normal'' state and an $S=0$ SDW state showing a spatial variation in the polarization as a consequence of broken spin symmetry in the internal coordinates[26]—indeed the interpretation of a SDW is still debated in the literature[21]—the SDFT calculations described here predict that the latter becomes more prevalent for even-$N$ systems as $\delta$ increases, particularly for small average particle densities.[17,20]

Another interesting, and in practice the simplest incidence we can focus on, is what happens to the $N=4$ ground state. The inset in Fig. 4 shows $\Delta_2(N=4)$ versus deformation up to $\delta=1.5$. Starting with the circular dot, Hund's first rule gives a total spin of $S=1$ for the triplet state favoring spin alignment of the two electrons in the second shell rather than a total spin of $S=0$ for the singlet state in which the spins are paired. As the deformation is initially increased, the energy separation between the two levels $(n_L,n_S)=(1,0)$ and $(0,1)$—the two originally degenerate levels $(n,l)=(0,1)$ and $(0,-1)$ in the second shell of the circular dot-increases [see (a) and (b) in Fig. 2], and so the spin-triplet state becomes progressively less favorable. $\Delta_2(4)$ continuously decreases with $\delta$, and at a value between 1.2 and 1.3, a spin-zero state (actually predicted by the SDFT described here to be a SDW) appears, i.e., a spin triplet-singlet transition is expected. For higher values of $\delta$ beyond this transition, $\Delta_2(N=4)$ starts to increase.

Other recent calculations employing numerical diagonalization for elliptical dots moderately deformed up to $\delta=2$ have also predicted that $\Delta_2(N)$ is sensitive to deformation, and that the spin-states can be modified.[14,15] Those calculations, for $N$ up to 10, and performed at 0 T with $E_Q=3$ meV, also reveal a spin triplet-singlet transition at $\delta\approx1.2$ for $N=4$, and, more generally, a consecutive filling of states by spin-up and spin-down electrons at higher deformation is favored.

Inspection of Fig. 3 gives values of $\Delta_2(N=4)$ for mesas *W*, *X*, *Y*, and *Z*, respectively of 3.1, 2.7, 3.1, and 2.5 meV. Whilst it is reassuring that these energies lie in the range predicted by SDFT, it is tempting to attribute, for a $\delta$ value equated to the $\beta$ value, the apparently anomalously low value for mesa *Z* to sample specific fluctuations, and say that the trend for mesas *W*, *X*, and *Y* is consistent with that predicted in Fig. 4 (inset), i.e., $N=4$ is a spin triplet for *W*, and a spin singlet for *X*, *Y*, and *Z*. However, as we do not really know $\delta$ for the elliptical dots, we can not even be confident that the actual $\delta$ values lie in the $\delta=1.0$ to 1.5 range, i.e., the values might be higher, or even that the order *X*, *Y*, and *Z* for increasing deformation as suggested by the $\beta$ values is correct. Fortunately, we can apply a *B* field, and as we will shortly show this goes a long way to resolving these difficult issues.

In case the actual $\delta$ values for the elliptical dots exceed 1.5, traces (g) and (h) in Fig. 4 respectively show $\Delta_2(N)$ for the higher deformation parameters $\delta=2$ and $\delta=3.2$. We have no reason to believe that $\delta$ experimentally will be exactly 2 or exactly 3.2, but the numbers are representative of the two situations where, respectively, many or no single-particle levels are degenerate at 0 T for noninteracting electrons, as illustrated by the spectra in Fig. 2. As expected, traces (g) and (h) show no circularlike shell structure, and no particularly large values of $\Delta_2(N)$. Indeed, apart from the ''classical'' background trend, i.e., $\Delta_2(N)$ increasing as $N$ decreases, there is little one can say about the traces except for $N>5$ there is a tendency for a weak even-odd oscillation in $\Delta_2(N)$, and this oscillation is perhaps clearer for larger $\delta$. The model here actually predicts small peaks for odd $N$, and small valleys for even $N$. For odd $N$, the spin state is nearly always $S=\frac{1}{2}$, and for even $N$ the spin-state is usually $S=0$ (SDW). At least for $\delta=2$, where in the single-particle picture there can be accidental degeneracies at 0 T [see Fig. 2 trace (c)], one might naively expect some nonzero even-$N$ spin states, but it is possible that in the model calculations, for the parameters given, the interactions modify the spectrum so dramatically that expected degeneracies are lifted reducing the visibility of any potential shell structure, e.g., $N=6$ and 10 are predicted here to be $S=0$ (SDW) rather than $S=1$ as might be expected from Hund's first rule. On the other hand, for $\delta=3.2$, where in the single-particle picture there are no accidental degeneracies at 0 T [see Fig. 2 trace (d)], perhaps surprisingly some nonzero even-$N$ spin states, for example for $N=12$ and 16, are predicted—this too may be due to interactions.

For *Y* and *Z*, the $\Delta_2(N)$ traces in Fig. 3 seem to show a weak tendency to oscillate between a slightly larger even-$N$ value, and a slightly smaller odd-$N$ value, and this oscillation seems clearer for *Y* than for *Z*. For the moment, we do not try to account for the clarity of this oscillation in dots *Y* and *Z*, but try to explain the origin of the oscillation, although we are now being forced to entertain the idea that $\delta$ for *Y* and *Z* may be much larger than 1.5. Starting from the over simple single-particle picture with a fixed confinement energy, and then including a constant interaction which is the same for even $N$ and odd $N$, a larger even-$N$ value is expected because only $\Delta_2$ (even $N$) can contain a finite contribution due to the single-particle energy level spacing. A slightly more advanced model, which is more realistic in principle, would be to have a constant interaction for odd $N$ (next electron added to an $S=\frac{1}{2}$ state already containing one electron) that is stronger than the constant interaction for even $N$ (next electron added to an empty state). If the former is larger than the latter plus the single-particle spacing (more likely in practice as $N$ increases), a weak tendency to oscillate between smaller even $N$ and larger odd $N$ could occur. This pattern is what the SDFT calculations predict in Fig. 4 for $\delta=2$ and $\delta=3.2$. The fact that $\Delta_2(N)$ for *Y* and *Z* is often a little larger for even $N$

than odd $N$ should not be taken to mean that the constant interaction model is more accurate. Rather the Coulomb interactions may not be so strong in practice, due to screening by the leads for example, as those in our model—a model that also does not include the self-consistent calculation of the electrostatic confining potential. Indeed, in the SDFT calculations of Lee *et al.*,[16] the electrostatic confining potential is much stronger (e.g., $E_S = 20$ meV, $E_L = 10$ meV), and they find that $\Delta_2(N)$ is generally a little larger for even $N$ than for odd $N$. Finally, we note that eventually, for a much stronger deformation (e.g., $\delta$ exceeding 10), the addition energy spectrum would become smoother as it tends towards that for a quasi-one-dimensional quantum wire.[20,27]

## V. MAGNETIC FIELD DEPENDENCE

Application of a magnetic field is a powerful tool with which to identify the quantum numbers of states in our vertical quantum dots.[6,10,11] Figure 2 instructively shows the expected evolution of the first ten single-particle energy levels with $B$ field up to 6 T for a circular dot ($\delta = 1$), and for elliptical dots with $\delta = 1.5$, 2, and 3.2. The energy level spectra are calculated according to the simple single-particle model employed by Madhav and Chakraborty[13] in which Coulomb interactions are neglected, and the confining potential is assumed to be perfectly parabolic. The spectrum for the circular dot is the familiar Darwin-Fock spectrum for a circular two-dimensional harmonic confining potential. The confinement energy for the circular dot $E_Q$ is taken to be 3 meV, in practice a reasonable average value in the few-electron limit, and is assumed to be independent of $N$. The confinement energies for the elliptical dots are simply derived from the relation $E_L E_S = E_Q E_Q$. For the case of the circle and the $\delta = 3.2$ ellipse, quantum numbers $(n,l)$ and $(n_L, n_S)$, respectively for some of the states we discuss are indicated. Each single-particle energy level can accommodate a spin-up and spin-down electron, so current peaks should normally come in pairs in a constant interaction model neglecting exchange.[13] ''Wiggles'' in the position of pairs of current peaks are expected because the $B$ field induces crossings between single-particle states.[6,10,13] The first lowest energy ''wiggle'' originates from the crossing marked by a black triangle in each of the four spectra. $\Delta_2$ (even $N$) is expected to be strongly dependent on $B$ field as it can contain contributions from single-particle energy level spacings, whereas $\Delta_2$ (odd $N$) is essentially independent of $B$ field at weak field, and is determined only by the effect of Coulomb repulsion. Any detailed discussion on the actual $B$-field dependence of the current peaks requires the inclusion of Coulomb interactions.[11] The four calculated spectra nevertheless clearly serve to demonstrate three simple points: (i) the $B$ field lifts all degeneracies present at 0 T at the ''magic'' deformations, e.g., $\delta = 1, 1.5, 2, \ldots$ ($\delta = 3.2$ is not a ''magic'' deformation); (ii) a $B$ field can always induce degeneracies at finite field when single-particle levels cross, provided the confinement potential is perfectly parabolic; and (iii) as $\delta$ increases, the single-particle energy level spacing generally decreases ($\leqslant E_L$).

Figure 5 shows the $B$-field dependence, for a weak field applied parallel to the current, of the Coulomb oscillation peak positions for the circular mesa $W$, (a), and the rectangular mesas $X$, $Y$, and $Z$, (b) to (d). The data consists of current vs $V_g$ traces taken at a very small bias ($\ll 1$ mV) at different $B$ fields at or below 0.3 K.

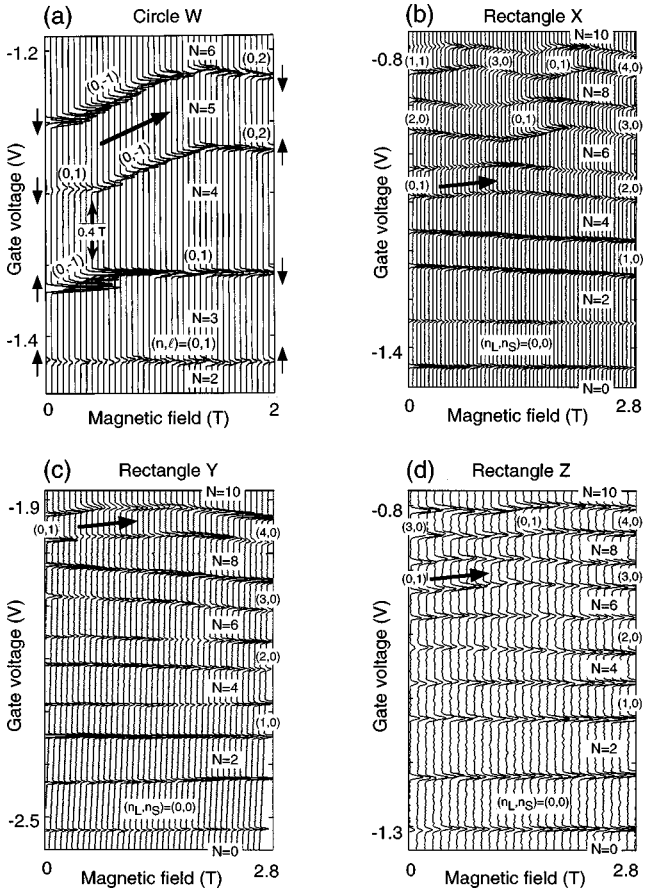


FIG. 5. Magnetic ($B$-) field dependence of the Coulomb oscillation peak positions for mesas $W$, $X$, $Y$, and $Z$, (a) to (d). The $B$ field is parallel to the current. The data consists of current versus $V_g$ traces for different $B$ fields, which are offset, and rotated by 90°. A less negative gate voltage corresponds to higher energy. For circular dot $W$, only the third, fourth, fifth, and sixth current peaks belonging to the second shell are shown. The unusual pairing of the third peak with the fifth, and the fourth peak with the sixth from 0 to 0.4 T as opposed to the more usual pairing for $B > 0.4$ T is evident, and is related to Hund's first rule. For $B > 0.4$ T, the fifth and sixth peaks, as a pair, first move up, as indicated by the thick arrow, and then start to move down at about 1.4 T due to the crossing between the single-particle states $(n,l) = (0,-1)$ and (0,2). The spins of the added electrons are shown pictorially at 0 and 2 T. For elliptical dots $X, Y, Z$, the first ten current peaks are shown. Peaks are paired, and there are no obvious deviations close to 0 T for $N = 4$ which can be attributed to exchange effects. Quantum numbers $(n_L, n_S)$ of the single-particle states are included, and the first up-moving pair of peaks is marked by a thick arrow. As deformation increases, the single-particle spectra in Fig. 2 show that this up-moving pair should move to higher $N$.

For circle $W$, only the third, fourth, fifth and sixth current peaks (belonging to the second shell at 0 T) are shown. The pairing of the third peak with the fifth peak, and the fourth peak with the sixth peak from 0 to 0.4 T, as opposed to the more usual pairing of the third peak with the fourth, and the fifth peak with the sixth (due to consecutive filling of electrons into spin-degenerate single-particle states) for $B$

$>0.4$ T, is a consequence of Hund's first rule: the $N=4$ state is a spin triplet so two parallel-spin electrons fill the two different but originally degenerate states $(n,l)=(0,1)$ and $(0,-1)$ in the half-filled second shell.[6,10] For $B>0.4$ T, the fifth and sixth peaks, as a pair, first move up, as indicated by the thick arrow, and then start to move down at about 1.4 T due to the crossing of the single-particle states $(n,l)=(0,-1)$ and (0,2). This lowest single-particle level crossing, which is also clear in Fig. 2(a), is marked by a black triangle. The spins of the added electrons are also shown pictorially at 0 and 2 T.

To explain why Hund's first rule is obeyed in a simple way, we can introduce an energy, $E_{EX}$, to represent the reduction in energy due to exchange between electrons in the half-filled second shell, and this is estimated to be about 0.7 meV for circle *W*.[6,10] The $N=4$ triplet state is thus lower in energy than the $N=4$ singlet-singlet state by $E_{EX}$, and as a consequence $\Delta_2(3)$, $\Delta_2(5)<\Delta_2(4)$ by about $2E_{EX}$. This exchange-related effect persists in a weak-*B* field as long as the splitting between states (0,1) and $(0,-1)$ is less than $E_{EX}$. At 1.4 T this splitting exceeds $E_{EX}$, and the ground state becomes a spin-singlet, i.e., there is a *B* field-induced triplet-singlet transition.

For rectangles *X*, *Y*, and *Z*, the first ten current peaks are shown in Figs. 5(b) to 5(d). Peaks are paired, and there are no obvious deviations close to 0 T for $N=4$, which can be attributed to exchange effects, i.e., Hund's first rule. Quantum numbers $(n_L,n_S)$ of the single-particle states are assigned, and the first up-moving pair of peaks is marked by a thick arrow. With increasing deformation, the first up-moving pair of peaks, and the lowest energy single-particle level crossing (identified by a black triangle in each of the Fig. 2 spectra) are simply expected to move systematically to higher *N* (or equivalently to higher energy).[13]

For the elliptical dots, normal peak pairing, even from 0 T, occurs so Hund's first rule is not obeyed. This suggests that the spin-state for $N=4$ is a singlet. The exchange effect is maximal for a circular dot at $N=4$ because the $(n,l)=(0,1)$ and $(0,-1)$ states are degenerate, but with deformation these states become the $(n_L,n_S)=(1,0)$ and (0,1) states in an elliptical dot which are split at 0 T. This energy splitting, $\gamma$, increases with $\delta$. If $\gamma<E_{EX}$ at 0 T, exchange can still operate to lower the energy, and thus the $N=4$ ground state remains a spin-triplet. On the other hand, if $\gamma>E_{EX}$ at 0 T, the energy gain due to exchange is not sufficiently large to compensate for the splitting, so normal pairing occurs. Thus, as $\delta$ increases, we can expect a triplet-singlet transition at some critical deformation.[12] Note that $E_{EX}$ itself decreases with increasing deformation, as it has its maximum value only when the orbitals involved have the same symmetry. This transition is clear in the inset of Fig. 4 according to SDFT, and has also been predicted by exact numerical diagonalization.[14,15] The tell-tail pattern in the trend of $\Delta_2(N=4)$ at 0 T with deformation should be an initial decrease while the state remains a spin triplet, a turning point at the transition, and a rise thereafter when the state is a spin singlet. As noted before, it is hard to judge from the absolute values of $\Delta_2(4)$ at 0 T alone shown in Fig. 3 whether the $N=4$ state is a triplet or singlet. $\Delta_2(4)$ can be relatively large either side of the turning point if either $E_{EX}$ or $\gamma$ is large, i.e., a large $\Delta_2(4)$ can mean Hund's first rule is operating for nearly degenerate states, or there is a large separation between nondegenerate states. This potential ambiguity is apparent when we see that $\Delta_2(4)$ for circle *W* and ellipse *Y* are essentially equal, so it is vitally important to examine carefully the *B*-field dependence. The absence of deviations to the normal peak pairing at $N=4$ in Fig. 5, traces (b) to (d), nevertheless does apparently confirm that $\delta$ is indeed greater than 1.2–1.3, which is in line with the $\beta$ values for mesas *X*, *Y*, and *Z*. For completeness, we note that normally we probe the spin states in our high-symmetry dot structures via the orbital effect with the *B* field parallel to the current. The spin-states in the elliptical dot *X* have also been confirmed directly by measuring the Zeeman effect alone by applying a *B* field perpendicular to the current, and the results are again consistent with a spin-singlet interpretation for $N=4$.[12]

The next most striking feature about traces (b) to (d) in Fig. 5 is the position of the first up-moving pair of peaks. For mesas *X*, *Y*, and *Z*, respectively, it is the third, fifth, and fourth pair of peaks. As revealed by the sequence of spectra in Fig. 2, in a simple single-particle picture, the first up-moving state is $(n_L,n_S)=(0,1)$, which is actually the lowest energy state of the second Landau level.[13] Inspection of these calculated spectra shows that this state is, in the weak-field limit, from the bottom, the third, fourth, and fifth state, respectively for $1\leqslant\delta<2$, $2\leqslant\delta<3$, and $3\leqslant\delta<4$. Thus, starting from no deformation, the first up-moving pair of peaks should go from the third to fourth, fourth to the fifth,... at certain ''magic'' deformations as $\delta$ is increased. Remembering that Coulomb effects are neglected in this simple picture, and that in practice $\delta$ is expected to vary with *N*, nonetheless, with these simple arguments it looks as if $1<\delta<2$ for *X*, $3<\delta<4$ for *Y*, $2<\delta<3$ for *Z*. If we believe this, then even though ellipses *X*, *Y*, and *Z* are all deformed beyond the triplet-singlet transition, we are forced to conclude the following: (i) $\delta$ can be much higher than that suggested by the $\beta$ values (especially for *Y* and *Z*); and (ii) the ordering given by increasing $\beta$ values may not reflect the true ordering in $\delta$, i.e., the deformation in *Y* seems to be stronger than in *Z*, so the true sequence may be *W*-*X*-*Z*-*Y* for the four mesas considered. Given our earlier comments, the former is not so unexpected since we have no independent way of measuring $\delta$, but the latter is perhaps more surprising.

If the true ordering of the ellipses is *X*, *Z*, and *Y*, even though the reason for the deformation in *Y* being stronger than in *Z* is unclear to us, at least other attributes of *Y* and *Z*, and trends in Figs. 3 and 5 are consistent with this interpretation. For instance, $\Delta_2(N=4)$ for a *W*-*X*-*Z*-*Y* ordering respectively of 3.1, 2.7, 2.5, and 3.1 meV is more in line with the predicted trend shown in the inset in Fig. 4, although the value for *Z* still seems a little low. This reordering does not contradict our earlier conclusion that, with the absence of deviations to normal pairing, $N=4$ is a spin-singlet state for all three ellipses. Thus, $\Delta_2(4)$ increases after the triplet-singlet transition, because with deformation the degeneracy of single-particle states is strongly lifted. The reversed ordering of ellipses *Y* and *Z*, as well as higher $\delta$ values than suggested by the $\beta$ values, also fits with the observations made earlier about traces (c) and (d) in Fig. 3, and traces (g) and (h) in Fig. 4. Both mesas show a tendency for $\Delta_2(N)$ to oscillate between slightly higher and slightly lower values,

respectively for even $N$ and odd $N$ and this seems more pronounced for $Y$ than $Z$.

## VI. CONCLUSIONS

We have experimentally and theoretically investigated the effect of ellipsoidal deformation on the shell structure, addition energies, and spin states in vertical quantum dot atoms on going from circular- to rectangular-shaped mesas. The familiar and distinctive shell structure as determined from the addition energy spectra at 0 T for the circular dot is absent in the elliptical dots, and even small deviations breaking circular symmetry have a dramatic effect. Measurements with a magnetic field applied parallel to current confirm that the $N=4$ spin state at 0 T has undergone a transition due to the moderate deformation: for the circular dot it is a spin-triplet in accordance with Hund's first rule when the second shell is half-filled, and for the elliptical dots it is a spin singlet. These observations are in agreement with recent theory, as well demonstrated here by the application of spin-density-functional theory at 0 T with a wide range of deformation parameters. The $B$-field dependence strongly suggests that the anisotropy of an elliptical dot in practice can be significantly higher than that given by simply considering the geometry of the mesa in which the dot is situated. In the future it will be interesting to experiment with even more strongly and extremely deformed dots (to clarify for instance the existence of $S=0$ SDW states), quasi-one-dimensional wirelike dots,[20,27] and possibly other exotically shaped dots, for example ring-shaped dots,[27] and triangular-shaped dots.[14,15] Finally, with these goals in mind, ultimately better control and *in situ* manipulation of the lateral potential geometry of a quantum dot is highly desirable, and this may be achieved by fully exploiting a multiple-gated vertical single-electron transistor we have recently developed.[28,29]

## ACKNOWLEDGMENTS

We would like to acknowledge the considerable assistance of Takashi Honda in the fabrication of the devices, and useful discussions with Yasuhiro Tokura and Hiroyuki Tamura. This work was partly supported by Grant No. 08247101 from the Ministry of Education, Science, Culture and Sports, Japan, the NEDO joint research program Grant No. (NTDP-98), the Academy of Finland, and the TMR program of the European Community under Contract No. ERBFMBICT972405. Our understanding of the circular dots has benefited from a long-term collaboration with Leo Kouwenhoven at the Delft University of Technology and his coworkers.

*Electronic address: austing@will.brl.ntt.co.jp

†Present address: Physics Department, University of Tokyo, 7-3-1 Hongo, Bunkyo-ku, Tokyo 113-0033, Japan.

‡Electronic address: reimann@phys.jyu.fi

[1] M. Weissbluth, *Atoms and Molecules* (Academic, New York, 1978).

[2] Å. Bohr and B. R. Mottelson, *Nuclear Structure* (Benjamin, New York, 1975), Vol. II.

[3] W. D. Knight, K. Clemenger, W. de Heer, W. A. Saunders, M. Chou, and M. L. Cohen, Phys. Rev. Lett. **52**, 2141 (1984). For reviews, see W. de Heer, Rev. Mod. Phys. **65**, 611 (1993) and M. Brack, *ibid.* **65**, 677 (1993).

[4] D. G. Austing, T. Honda, Y. Tokura, and S. Tarucha, Jpn. J. Appl. Phys., Part 1 **34**, 1320 (1995).

[5] D. G. Austing, T. Honda, and S. Tarucha, Semicond. Sci. Technol. **11**, 388 (1996).

[6] S. Tarucha, D. G. Austing, T. Honda, R. J. van der Hage, and L. P. Kouwenhoven, Jpn. J. Appl. Phys., Part 1 **36**, 3917 (1997).

[7] M. A. Kastner, Phys. Today **46** (1), 24 (1993).

[8] U. Meirav and E. B. Foxman, Semicond. Sci. Technol. **11**, 255 (1996).

[9] R. C. Ashoori, Nature **379**, 413 (1996).

[10] S. Tarucha, D. G. Austing, T. Honda, R. J. van der Hage, and L. P. Kouwenhoven, Phys. Rev. Lett. **77**, 3613 (1996).

[11] L. P. Kouwenhoven, T. H. Oosterkamp, M. W. S. Danoesastro, M. Eto, D. G. Austing, T. Honda, and S. Tarucha, Science **278**, 1788 (1997).

[12] S. Sasaki, D. G. Austing, and S. Tarucha, Physica B **256-258**, 157 (1998).

[13] A. V. Madhav and T. Chakraborty, Phys. Rev. B **49**, 8163 (1994); See also, P. A. Maksym, Physica B **249-251**, 233 (1998).

[14] T. Ezaki, N. Mori, and C. Hamaguchi, Phys. Rev. B **56**, 6428 (1997).

[15] T. Ezaki, Y. Sugimoto, N. Mori, and C. Hamaguchi, Semicond. Sci. Technol. **13**, A1 (1998).

[16] I-H. Lee, V. Rao, R. M. Martin, and J-P Leburton, Phys. Rev. B **57**, 9035 (1998).

[17] M. Koskinen, M. Manninen, and S. M. Reimann, Phys. Rev. Lett. **79**, 1389 (1997).

[18] O. Steffens, U. Rössler, and M. Suhrke, Europhys. Lett. **42**, 529 (1998).

[19] E. Lipparini and L. Serra, Phys. Rev. B **57**, R6830 (1998).

[20] S. M. Reimann, M. Koskinen, J. Kolehmainen, M. Manninen, D. G. Austing, and S. Tarucha, Euro. J. Phys. D (to be published).

[21] K. Hirose and N. S. Wingreen, Phys. Rev. B **59**, 4604 (1999).

[22] W. Kohn and L. J. Sham, Phys. Rev. **140**, A1133 (1965).

[23] B. Tanatar and D. M. Ceperley, Phys. Rev. B **39**, 5005 (1989).

[24] D. G. Austing, Y. Tokura, T. Honda, S. Tarucha, M. Danoesastro, J. Janssen, T. H. Oosterkamp, and L. P. Kouwenhoven, Jpn. J. Appl. Phys., Part 1 **38**, 372 (1999).

[25] S. M. Reimann, M. Koskinen, P. E. Lindelof, and M. Manninen, Physica E **2**, 648 (1998).

[26] P. Ring and P. Schuck, *The Nuclear Many-body Problem* (Springer, New York, 1980).

[27] S. M. Reimann, M. Koskinen, and M. Manninen, Phys. Rev. B **59**, 1613 (1999).

[28] D. G. Austing, T. Honda, and S. Tarucha, Physica E **2**, 583 (1998).

[29] D. G. Austing, T. Honda, and S. Tarucha, Semicond. Sci. Technol. **12**, 631 (1997).